Published in final edited form as:
Magn Reson Med. 2005 December ; 54(6): 1557–1561.

Real-Time Blood Flow Imaging Using Autocalibrated Spiral Sensitivity Encoding

Reza Nezafat[1,2,*], **Peter Kellman**[2], **J. Andrew Derbyshire**[2], and **Elliot R. McVeigh**[1,2]

1*Department of Biomedical Engineering, Johns Hopkins University, Baltimore, Maryland, USA.*

2*Laboratory of Cardiac Energetics, National Institutes of Health, National Heart, Lung and Blood Institute, Department of Health and Human Services, Bethesda, Maryland, USA.*

Abstract

A novel spiral phase contrast (PC) technique was developed for high temporal resolution imaging of blood flow without cardiac gating. An autocalibrated spiral sensitivity encoding (SENSE) method is introduced and used to reconstruct PC images. Numerical simulations and a flow phantom study were performed to validate the technique. To study the accuracy of the flow measurement in vivo, a high-resolution cardiac experiment was performed and a subset of undersampled SENSE reconstructed data were reconstructed. Good agreement between the velocity measurement from the fully-sampled and undersampled data was achieved. Real-time experiments were performed to measure blood velocity in the ascending aorta and aortic valve, and during a Valsalva maneuver. The results demonstrate the potential of this technique for real-time flow imaging.

Keywords

phase contrast; real time imaging; spiral sampling; parallel imaging; auto-calibrated field map

Phase contrast (PC) MRI can be used to image rapid variations in blood flow in the cardiovascular system (1-5). Improved acquisition efficiency can be used to improve the accuracy of real-time PC-MRI by achieving a higher spatial or temporal resolution. One way to improve the acquisition efficiency is to use non-Cartesian trajectories, such as spiral sampling employing the maximum available gradient hardware for faster acquisition (2-4). Nayak et al. (2) used the improvement of imaging hardware to acquire images sampled with spiral trajectory with an in-plane resolution of 2.4 mm on a 20-cm field of view (FOV) with temporal resolution of 180 ms. However, despite the use of efficient sampling trajectories, real-time PC-MRI still suffers from low spatial and temporal image resolution.

Another approach to further improve the resolution is to acquire only a fraction of required raw *k*-space data for a given image resolution. Parallel imaging can be used to estimate the unacquired data by exploiting the coil sensitivity maps at the cost of signal-to-noise ratio (SNR; a loss of at least $\sqrt{R}$ in SNR loss for acceleration rate R) (6,7). Typically, parallel imaging is applied to Cartesian-sampled acquisitions due to the simplicity of the inverse solution. The accuracy and reproducibility of blood flow velocity measurements using SENSE reconstruction with Cartesian sampling at different reduction factors were studied recently, and an accurate estimate of flow measurement was predicted (8). For arbitrary sampling trajectories, conjugate gradient SENSE reconstruction has been proposed to suppress the artifacts arising from undersampled data (9).

*Correspondence to: Reza Nezafat, Laboratory of Cardiac Energetics, National Institutes of Health, National Heart, Lung and Blood Institute, 10 Center Drive, MSC-1061, Building 10, Room B1 D412, Bethesda, MD 20892-1061. E-mail: nezafatr@nih.gov

In the present study we combined PC imaging using spiral sampling with SENSE reconstruction to achieve a further improvement in temporal resolution for flow imaging. Furthermore, an autocalibrated acquisition scheme previously employed for Cartesian sampling is extended for use with spiral sampling (10).

MATERIALS AND METHODS

Imaging Sequence and Materials

We developed the spiral PC pulse sequence by adding a pair of bipolar gradients with the desired first-moment difference to the standard spiral sequence (11,12). Furthermore, the refocusing lobe in the slice-selection gradient was also combined with the flow-encoding bipolar gradient to reduce the length of the echo delay. When a magnitude image in addition to the flow image was required, a water-selective spectral-spatial pulse was used to suppress fat signals and reduce off-resonance blurring (13). A schematic of the pulse sequence is shown in Fig. 1. A randomized spiral interleave ordering was used in all real-time experiments to reduce the motion artifacts resulting from the acquisition ordering of spiral interleaves (14). Two low-resolution, single-shot images with different echo times (TEs) were acquired at the end of the scans for off-resonance field map calculation and correction (15). All of the MR experiments were performed on a GE Signa Excite 1.5T MRI system (GE, Waukesha, WI, USA) with twin gradients (maximum gradient amplitude = 4 G/cm; maximum gradient slew rate = 150 G/cm/ms) using an eight-channel cardiac phased-array coil (Nova Medical, Wilmington, MA, USA) for signal detection. All images were reconstructed offline using Matlab (The MathWorks, Natick, MA, USA). All normal volunteers were imaged after they provided consent, as approved by the NHLBI institutional review board. Breath-held experiments were performed on all in vivo measurements except the Valsalva maneuver study.

Spiral SENSE Reconstruction

Image reconstruction was carried out using an iterative conjugate gradient SENSE reconstruction (9) with an improvement in reconstruction time proposed by Wajer and Pruessmann (16). The raw spiral data were resampled into a denser Cartesian grid to reduce aliasing and to allow less apodization. The gridding procedure involved a convolution with a 5×5 Kaiser-Bessel kernel followed by deapodization in the image domain (17). An extra noise scan was acquired at the start of each study to prewhiten the data in the SENSE reconstruction (9). The simulations used uncorrelated noise and therefore did not require prewhitening.

To eliminate the acquisition of extra body- and multicoil reference scans, we proposed an autocalibrated SENSE acquisition scheme that is an extension of our previously shown autocalibrated technique for Cartesian imaging (10). The method provides adaptive B_1 maps that can track changes that may arise, for example, from respiratory motion during the cardiac cycle. In this technique, the spiral arms are interleaved in consecutive phases of the cardiac cycle and the pattern is repeated after R cardiac phases (the acceleration rate). Spiral interleaves for the acquisition of a fully sampled unaliased image are divided into different groups. The number of groups is equal to the acceleration rate of the imaging experiments. These groups are acquired consecutively and the data acquired in each group are used to reconstruct a particular cardiac phase. A full-FOV unaliased image is reconstructed by integrating the raw data across several phases. To calculate a relative coil sensitivity map, the temporally-filtered, alias-free, full-FOV images in each phase are normalized by the root sum of squared magnitudes of the multiple coil images. To optimize SNR in the combined image and suppress motion artifacts, a spatial matched filter is used in the reconstruction of the coil sensitivity maps (18). Local correlation statistics for each voxel are derived by cross-products over a local region in the complex image. The B_1 maps are reconstructed by calculating the eigenvector that corresponds to the maximum eigenvalue for each voxel.

Numerical Simulations and Phantom Validation

A numerical simulation study was performed to investigate the accuracy of the voxel phase of phantom images reconstructed with conjugate gradient SENSE. For validation of the estimated phase, we measured and compared the phase from the complex MR image of a stationary circular phantom reconstructed using conjugate gradient SENSE with the true phase of the phantom. Fifty-eight uniformly spaced phases, ranging between $-\pi$ and π, were added to the phantom, which originally had zero phase, yielding a series of test images with different phase values. The resulting images were weighted with the known sensitivity map of eight coils, calculated using Biot-Savart's law, to simulate a multicoil acquisition. The images were transformed into *k*-space by inverse Fourier transform and resampled onto a spiral trajectory using inverse gridding. The spiral *k*-space consisted of six interleaves and 1024 points per interleave, and an image size of 128 × 128. Images were reconstructed from a subset of the spiral interleaves corresponding to acceleration rates of 2 and 3 using conjugate gradient SENSE. The mean and standard deviation (SD) of the estimated phase were measured and compared with the added phase.

For flow validation experiments, volumetric through-plane flow rates were measured in a constant flow rate tube phantom. Experiments were performed with five flow rates ranging from 3.92 mL/s to 27.48 mL/s. The imaging parameters were as follows: TR = 24.3 ms, V_{enc} = 100 cm/s, $\theta = 30°$, slice thickness = 10 mm, FOV = 28 cm × 28 cm, BW = ±125 kHz, 2096 readout points, and 12 spiral interleaves.

In Vivo Studies

For in vivo validation, imaging studies measuring through-plane blood flow in the ascending aorta of normal human volunteers were performed. Gated cine flow scans were acquired for the measurement of blood flow. Breath-hold cine PC images were acquired in the ascending aorta with spiral sampling with the following parameters: TR = 15.9 ms, V_{enc} = 170 cm/s, $\theta = 30°$, FOV = 30 cm × 30 cm, BW = ± 125 kHz, slice thickness = 10 mm. A spatial resolution of 1.8 mm × 1.8mm was achieved using 12 spiral interleaves with an image matrix of 256 × 256. A single interleaf per segment (i.e., one TR per cardiac phase) was used to achieve a temporal resolution of 31.8 ms. Subsets of interleaves corresponding to undersampling rates of 2, 3, and 4 were chosen for image reconstruction.

Blood flow rate through the ascending aorta can be used to measure the cardiac output of patients during a stress tests. Here, real-time blood flow acquisitions were performed for measurements of blood flow in the ascending aorta. The acquisition parameters were as follows: TR = 15.2 ms, TE = 2.3 ms, V_{enc} = 150 cm/s, $\theta = 30°$, FOV = 34 cm, BW = ±125 kHz, and slice thickness = 10 mm. The fully sampled *k*-space consists of eight interleaves; however, two interleaves were acquired (i.e., acceleration rate of 4) with 2048 readout points in each interleave. A temporal resolution of 60.8 ms was achieved for acquisition of both bipolar experiments with these imaging parameters.

The severity of aortic stenosis can be visualized by monitoring the blood flow velocity across the aortic valve. Blood flow through the aortic valve was imaged with no cardiac gating, achieving a temporal resolution of 91.2 ms and an in-plane spatial resolution of 1.8 × 1.8 mm^2. An acceleration rate $R = 3$ was used with the following parameters: TR = 15.2 ms, V_{enc} = 150 cm/s, $\theta = 30°$, FOV = 26 cm, BW = ±125 kHz, and slice thickness = 10 mm with an image matrix of 256 × 256.

The blood flow was imaged in the abdominal aorta and inferior vena cava (IVC) in an axial slice below the renal arteries during a Valsalva maneuver. The volunteers performed a forced expiration for a period of 10–15 s followed by normal breathing. The typical acquisition

parameters were as follows: TR = 33.8 ms, TE = 3.1 ms, V_{enc} = 200 cm/s, θ = 30°, FOV = 40 cm, BW = ±125 kHz, with an acceleration rate of 3 for a total of six interleaves. A spectral-spatial RF pulse was used for these experiments to excite only water.

RESULTS

We validated the phase estimation of the stationary phantom by comparing the reconstructed phase for various linearly-spaced phase increments. Fifteen regions of interest (ROIs) in different spatial locations in the phantom were selected to calculate the mean and SD of the reconstructed phase. A linear correlation analysis was performed that yielded an $r > 0.9877$ and a slope of 0.9781 for rate 2 undersampling. The correlation analysis results in an $r > 0.9879$ and a slope of 0.9765 for rate 3 undersampling. Average through-plane flow velocities were calculated by averaging the velocity through an ROI placed on the lumen of the tube. A linear correlation analysis was performed for five different flow velocities with different undersampling rates. The average flow velocity measured from PC images reconstructed with acceleration rates of 2, 3, and 4 yielded an $r > 0.96$, 0.94, and 0.90, and a slope of 0.99, 0.99, and 0.99, respectively.

Cardiac-gated PC images were reconstructed from the subset of the interleaves corresponding to acceleration rates of 1, 2, 3, and 4. The acceleration rate $R = 1$ corresponded to B_1-map-weighted image reconstruction. The measured flow rate within the ascending aorta is shown in Fig. 2 for different undersampling rates. The average through-plane blood flow velocity in the ascending aorta acquired over a time period spanning several heartbeats is shown in Fig. 3. The average blood flow velocity was calculated over an ROI placed within the vessel, and the motion of the vessel during the cardiac cycle was compensated for by manual ROI registration. The low SNR in the low velocity flow phases shows a more nonperiodic flow pattern. The in vivo real-time velocity image through the aortic valve is shown in Fig. 4 along with the magnitude image. The magnitude image was acquired in a separate acquisition using spectral-spatial pulses to reduce the off-resonance effect and suppress fat (for display purposes only). The blood flow velocity of a sample voxel through the valve is shown on the velocity map image, which shows the periodic closing and opening cycle of the valve over multiple cardiac cycles. The velocity of the blood flow for a cardiac cycle was also measured with a gated sequence, and the results showed close agreement with the real-time acquired flow measurements. The magnitude images and velocity maps during different phases of the Valsalva maneuver are shown in Fig. 5. The images show the through-plane blood flow through the IVC and aorta before, during, and after the forced expiration during the Valsalva maneuver. The increase in thoracic pressure caused a total collapse of the IVC and no return of blood flow during the forced expiration, as shown in Fig. 5b. There was a sudden increase in the blood flow in the IVC after forced expiration (Fig. 5c), followed by a decrease toward normal velocity (Fig. 5d).

DISCUSSION

We have demonstrated a technique for measuring real-time flow velocity with improved temporal resolution for an image of a given spatial resolution. The gain in temporal resolution comes from the SENSE acceleration factor used in the image acquisition and reconstruction. The increase in efficiency can be used to improve spatial resolution by prescribing an image with a higher number of readouts (i.e., increasing the number of the spiral interleaves or readout), and the increased imaging time required for acquisition of the image is then offset by using SENSE. Compared to other reduced-FOV methods, such as unaliasing by Fourier-encoding the overlaps using the temporal dimension (UNFOLD) (19) or view sharing, SENSE reconstruction does not have temporal filtering effects.

Imaging the blood flow with high spatial resolution decreases the partial volume effects that arise from partial occupancy of the voxels with static spins. Furthermore, the reduced acquisition time decreases underestimation of the peak velocity due to averaging over shorter period of time around the peak amplitude. The achieved imaging resolution in this study is significantly higher than that obtained in previous real-time flow imaging studies (1,2,4,5). With SENSE, the temporal resolution is improved by at least a factor of 3 compared to a non-accelerated acquisition. However, it is difficult to make a fair comparison of acquisition efficiency in flow imaging acquired with different sampling techniques, such as echo-planar, radial, and spiral imaging, because of the various imaging parameters and imaging artifacts that can affect the accuracy of the flow quantification. Further study is required to compare the acquisition efficiency of the SENSE-accelerated spiral with that achieved in a reduced-FOV study using a single surface coil, because of the different SNR losses and gains obtained by prescribing a smaller FOV.

Further investigations are also needed to quantify the local SNR penalty from reconstructing the undersampled spiral *k*-space data. In the flow quantification, this SNR loss is manifested as variations in the peak velocity and, more distinctively, in low flow velocity. A higher number of mutually distinctive receive channels and better penetration depth will significantly improve the SNR of the reconstructed image and allow higher acceleration rates.

Image reconstruction in this study was performed offline after the scanning procedures were completed. Low temporal resolution images were reconstructed online using all the spiral interleaves required for a single phase to obtain real-time feedback during scanning. A system for real-time reconstruction of flow to generate real-time color-coded images (as is done in ultrasound imaging) should be feasible, but was not studied in this work.

CONCLUSIONS

We have demonstrated a technique that provides improved temporal resolution imaging of blood flow without cardiac gating. The temporal resolution of the flow images was accelerated by a factor of at least 3 with no cardiac gating signal, and with preserved spatial resolution and acceptable image quality. The adaptive B_1 map calculation from the raw data eliminates the need for an extra body-coil scan. The results demonstrate the potential of this technique for real-time flow imaging with improved spatial and temporal resolution.

ACKNOWLEDGMENTS

We thank Daniel Herzka, Luis Gutierrez, Richard B. Thompson, and Daniel Ennis for helpful discussions and editing the manuscript. Reza Nezafat was financially supported by a predoctoral visiting fellowship at the National Institutes of Health.

REFERENCES

1. Riederer S, Wright R, Ehman R, Rossman P, Holsinger-Bampton A, Hangiandreou N, Grimm R. Real-time interactive color flow MR imaging. Radiology 1991;181:33–39. [PubMed: 1887053]
2. Nayak K, Pauly J, Kerr A, Hu B, Nishimura D. Real-time color flow MRI. Magn Reson Med 2000;43:251–258. [PubMed: 10680689]
3. Pike G, Meyer C, Brosnan T, Pelc N. Magnetic resonance velocity imaging using a fast spiral phase contrast sequence. Magn Reson Med 1994;32:476–483. [PubMed: 7997113]
4. Gatehouse P, Firmin D, Collins S, Longmore D. Real time blood flow imaging by spiral scan phase velocity mapping. Magn Reson Med 1994;31:504–512. [PubMed: 8015403]
5. Klein C, Schalla S, Schnackenburg B, Bornstedt A, Fleck E, Nagel E. Magnetic resonance flow measurements in real time: comparison with a standard gradient-echo technique. J Magn Reson Imaging 2001;14:306–310. [PubMed: 11536408]

6. Sodickson D, Manning W. Simultaneous acquisition of spatial harmonics (SMASH): fast imaging with radiofrequency coil arrays. Magn Reson Med 1997;38:591–603. [PubMed: 9324327]
7. Pruessmann K, Weiger M, Scheidegger M, Boesiger P. SENSE: sensitivity encoding for fast MRI. Magn Reson Med 1999;42:952–962. [PubMed: 10542355]
8. Thunberg P, Karlsson M, Wigstrom L. Accuracy and reproducibility in phase contrast imaging using SENSE. Magn Reson Med 2003;50:1061–1068. [PubMed: 14587017]
9. Pruessmann KP, Weiger M, Bornert P. Advances in sensitivity encoding with arbitrary k-space trajectories. Magn Reson Med 2001;46:638–651. [PubMed: 11590639]
10. Kellman P, Epstein F, McVeigh E. Adaptive sensitivity encoding incorporating temporal filtering (TSENSE). Magn Reson Med 2001;45:846–852. [PubMed: 11323811]
11. Meyer C, Hu B, Nishimura D, Macovski A. Fast spiral coronary artery imaging. Magn Reson Med 1992;28:202–213. [PubMed: 1461123]
12. Bernstein M, Shimakawa A, Pelc N. Minimizing TE in moment-nulled or flow-encoded two-and three-dimensional gradient-echo imaging. J Magn Reson Imaging 1992;2:583–588. [PubMed: 1392252]
13. Meyer C, Pauly J, Macovski A, Nishimura D. Simultaneous spatial and spectral selective excitation. Magn Reson Med 1990;15:287–304. [PubMed: 2392053]
14. Pipe J, Ahunbay E, Menon P. Effects of interleaf order for spiral MRI of dynamic processes. Magn Reson Med 1999;41:417–422. [PubMed: 10080293]
15. Irarrazabal P, Meyer C, Nishimura D, Macovski A. Inhomogeneity correction using an estimated linear field map. Magn Reson Med 1996;35:278–282. [PubMed: 8622593]
16. Wajer FTAW, Pruessmann KP. Major speedup of reconstruction for sensitivity encoding with arbitrary trajectories. Proc Intl Soc Mag Reson Med 2001;9:767.
17. Jackson J, Meyer CH, Nishimura D, Macovski A. Selection of convolution function for Fourier inversion using gridding. IEEE Trans Med Imaging 1991;10:473–478. [PubMed: 18222850]
18. Walsh D, Gmitro A, Marcellin M. Adaptive reconstruction of phased array MR imagery. Magn Reson Med 2000;43:682–690. [PubMed: 10800033]
19. Madore B, Glover G, Pelc N. Unaliasing by Fourier-encoding the overlaps using the temporal dimension (UNFOLD), applied to cardiac imaging and fMRI. Magn Reson Med 1999;42:813–828. [PubMed: 10542340]

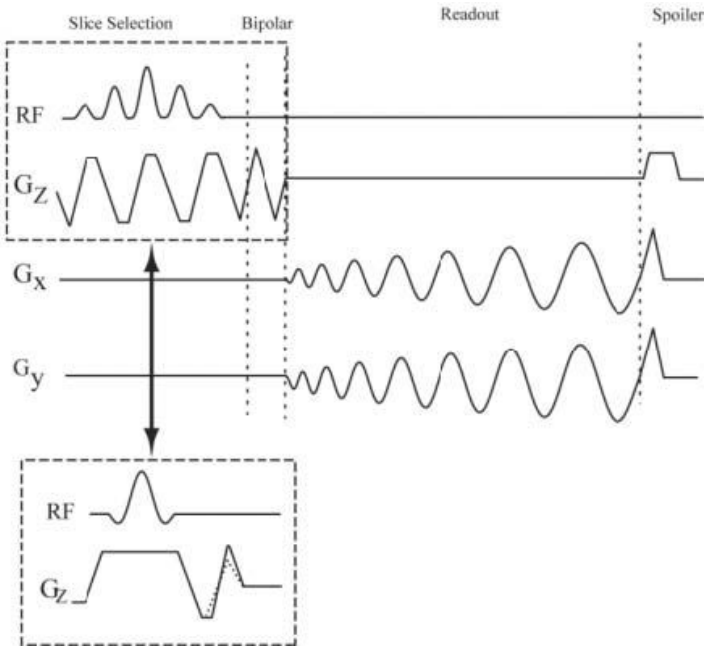

FIG. 1.

Spiral PC pulse sequence with and without selective spectral-spatial RF pulse. When both a magnitude image and a flow image are required, a water-selective, spectral-spatial pulse is used. For flow imaging experiments without a spectral-spatial selection pulse, the nonsymmetric bipolar gradients were combined with the refocusing lobe of the slice-select gradient. The dashed lines overlaid on the flow-encoding gradient represent the alternate TR bipolar gradient.

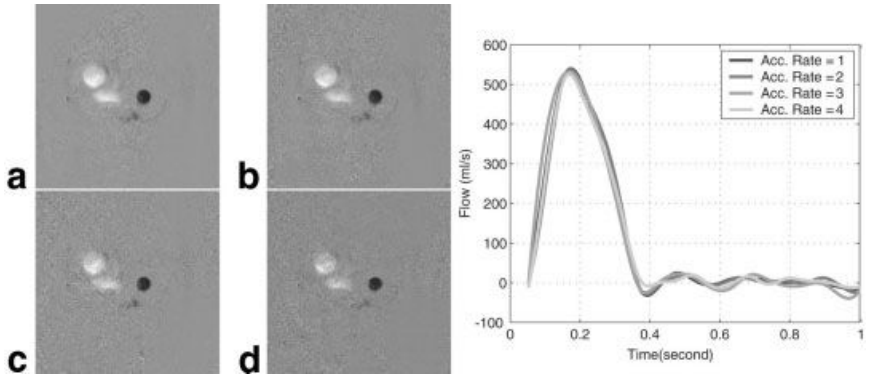

FIG. 2.

Gated flow images through the ascending aorta calculated from an ROI placed in the aorta for acceleration rates 2, 3, and 4 in comparison with a B_1-map-weighted flow image. **a:** Flow image during late systole reconstructed without acceleration and from acceleration rates 2, 3, and 4, respectively, for **b–d**. Flow image quality and quantitative measurement of flow velocity are comparable for each reconstruction.

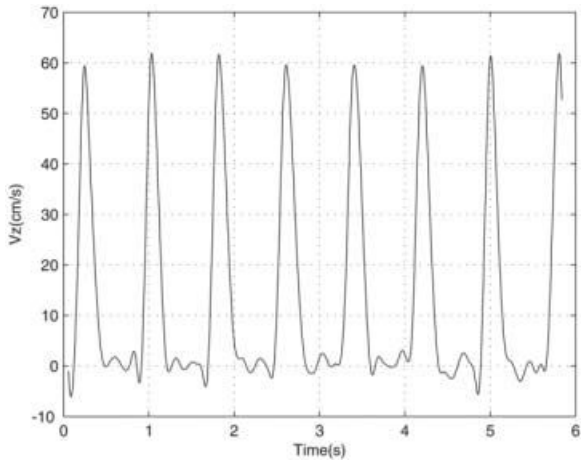

FIG. 3.

Real-time acquired average through-plane blood flow velocity V_z (cm/s) within the ascending aorta. The flow velocity images were calculated from a series of undersampled images acquired with an acceleration rate $R = 4$ using autocalibrated spiral SENSE with a temporal resolution of 60.8 ms. A reproducible peak velocity was observed, while the low velocity flow does not show a periodic pattern, due to lower SNR.

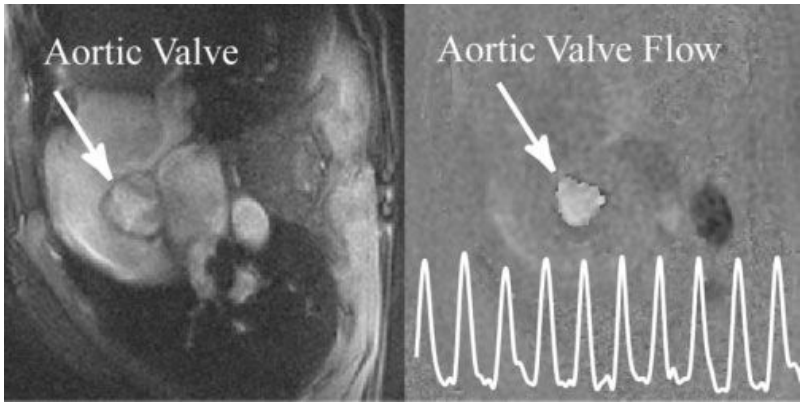

FIG. 4.

Real-time, through-plane image of blood flow in the aortic valve acquired with a temporal resolution of 91.2 ms and an in-plane resolution of $1.8 \times 1.8\ mm^2$. The trace on the PC image shows the calculated through-plane velocity through an ROI placed in the middle of the valve.

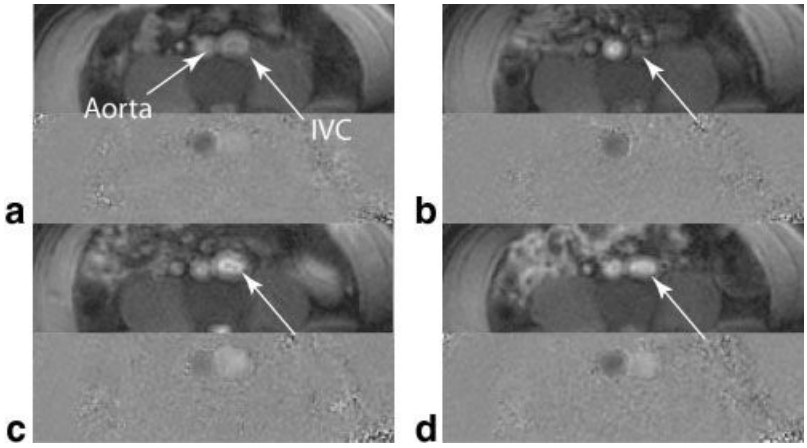

FIG. 5.

Imaging of the blood flow in an axial infrarenal slice during the Valsalva maneuver: (**a**) magnitude and velocity map before the first phase of the maneuver, (**b**) during the forced expiration, (**c**) just after release, and (**d**) 5 s after release approaching the normal status. The arrows show the IVC during the process, and a collapse of the IVC lumen is visible in the forced expiration phase with no flow.